Supporting Information for

Alternative Alcohol-soluble Conjugated Small Molecule Electrolytes for High-efficiency Inverted Polymer Solar Cells

Yueqin Shi[1], Licheng Tan[1,2], Lie Chen[1,2], Yiwang Chen*[1,2]

[1]School of Materials Science and Engineering/Institute of Polymers, Nanchang University, 999 Xuefu Avenue, Nanchang 330031, China; [2]Jiangxi Provincial Key Laboratory of New Energy Chemistry, College of Chemistry, Nanchang University, 999 Xuefu Avenue, Nanchang 330031, China

Materials

3,6-Dithiophene-2-yl-2,5-dihydro-pyrrolo[3,4-*c*]pyrrole-1,4-dione, 1-bromo-2-ethylhexane, 4-(4,4,5,5-tetramethyl-1,3,2-dioxaborolan-2-yl)benzoic acid, ($Pd(PPh_3)_4$), bromosuccinimide (NBS), anhydrous potassium carbonate (K_2CO_3), anhydrous magnesium sulfate ($MgSO_4$), 1,2-dichlorobenzene (o-DCB, spectrum pure), chloroform ($CHCl_3$), dimethyl formamide (DMF) and methanol (spectrum pure) were purchased from Alfa Aesar and used as received without any further purification. Tetrahydrofuran (THF) and hexane was dried over sodium. And other chemicals were obtained from Shanghai Reagent Co., Ltd., and used as received. Regioregular P3HT (Mw = 48300 g/mol, head-to-tail, regioregularity > 90%), [6,6]-phenyl-C_{61}-butyric acid methyl ester (PCBM) (99.5% purity), and MoO_3 were purchased from Rieke Metals, Inc. and Nano-C. Poly{4,8-bis[(2-ethylhexyl)oxy]benzo[1,2-b:4,5-b']dithiophene-2,6-diyl-alt-3-fluoro-2-[(2-ethylhexyl)carbonyl]thieno[3,4-b]thiophene-4,6-diyl} (PTB7) and [6,6]-phenyl-C_{71}-butyric acid methyl ester ($PC_{71}BM$) were used. Indium-tin oxide (ITO) glass was obtained from Delta Technologies Limited, while PEDOT:PSS (Baytron PAl4083) was purchased from Bayer Inc.

Synthesis of 3,6-bis-(2-ethylhexyl)-3,6-dithiophen-2-yl-2,5-dihydro-pyrrolo[3,4-

* Corresponding author. Tel.: +86 791 83968703; fax: +86 791 83969561. *E-mail address*: ywchen@ncu.edu.cn (Y. Chen).

***c*]pyrrole-1,4-dione**

To a stirred solution of 3,6-dithiophene-2-yl-2,5-dihydro-pyrrolo[3,4-*c*]pyrrole-1,4-dione (0.483 g, 1.61 mmol) and 1-bromo-2-ethylhexane (0.622 g, 3.22 mmol) in dry dimethyl formamide (DMF, 80 mL) and aqueous K_2CO_3 (1.38 g; N_2 bubbled before use), the mixture was vigorously stirred for 24 h at 100 ºC. After cooling to room temperature, the reaction mixture was poured into water, and then extracted with $CHCl_3$. The combined organic layers was washed with water, and dried over anhydrous $MgSO_4$. Then, the crude product was purified by column chromato-graphically from $CHCl_3$, and dried under vacuum.

Synthesis of 3,6-bis-(5-bromo-thiophen-2-yl)-2,5-bis-(2-ethylhexyl)-2,5-dihydro-pyrrolo[3,4-*c*]pyrrole-1,4-dione

The crude product (6.812 g, 1.3×10^{-2} mol) and N-bromosuccinimide (NBS, 4.6 g, 2.6×10^{-2} mol) were dissolved in 30 mL $CHCl_3$ in a dried 250 mL round bottom flask wrapped in aluminum foil. The flask was degassed with nitrogen for 15 min before being sealed under a nitrogen atmosphere. The reaction was run at room temperature overnight. The solution was filtered to remove residual NBS, then $CHCl_3$ was removed by rotary evaporation. The product was eluted over silica gel using $CHCl_3$. The solvent was removed by rotary evaporation to yield the desired product.

Synthesis of 3,6-bis-(5- benzoic acid-thiophen-2-yl)-2,5-bis-(2-ethylhexyl)-2,5-dihydro-pyrrolo[3,4-*c*]pyrrole-1,4-dione (DPP-COOH) [1]

To a stirred solution of 3,6-bis-(5-bromo-thiophen-2-yl)-2,5-bis-(2-ethylhexyl)-2,5-dihydro-pyrrolo[3,4-*c*]pyrrole-1,4-dione (1.098 g, 1.61 mmol) and 4-(4,4,5,5-tetramethyl-1,3,2-dioxaborolan-2-yl)benzoic acid (0.7981 g, 3.22 mmol) in dry tetrahydrofuran (THF, 80 mL) were added $Pd(PPh_3)_4$ (0.075 g, 0.064 mmol) and aqueous K_2CO_3 (2.0 M, 5 mL; N_2 bubbled before use), the mixture was vigorously stirred for 24 h at 55 ºC. After cooling to room temperature, the reaction mixture was poured into water, and then extracted with $CHCl_3$. After filtration and evaporation, the crude product was purified by column chromato-graphically with ethyl acetate, and

dried under vacuum to afford a dark violet solid. The product was soluble in alcohol but insoluble in chloroform. ^{1}H NMR (500 MHz, DMSO): δ 10.2 (1H), 8.97 (d, J=4.0 Hz, 2H), 7.59 (d, J=8.5 Hz, 4H), 7.43 (d, J=4.0 Hz, 2H), 7.23 (d, J=8.0 Hz, 4H), 3.83-3.73 (m, 2H), 1.77-1.62 (m, 8H), 1.37-1.20 (m, 12H), 0.93-0.85 (m, 12H).

Preparation of ZnO thin film

ZnO thin films coated on the top of ITO glass were obtained from ZnO precursor solution by sol-gel method[2]. The ZnO precursor was prepared by dissolving zinc acetate dihudrate ($Zn(CH_3COO)_2{\cdot}2H_2O$, Aldrich, 1.0 g) and ethanolamine ($NH_2CH_2CH_2OH$, Aldrich, 0.28 g) in 2-methoxyethanol ($CH_3OCH_2CH_2OH$, Aldrich, 10 mL), under vigorous stirring for 12 h for the hydrolysis reaction in air.

Fabrication of inverted BHJ device

Two types of inverted BHJ solar cells were fabricated on ITO-coated glass substrates. The ITO-coated glass substrates were first cleaned with acetone, detergent, ultrasonicated in water and isopropyl alcohol subsequently. The ZnO precursor solution was spin-cast on top of the ITO substrate. Then, the films were thermal-annealed at 235 ºC for 1h in air. For this inverted BHJ solar cells with ZnO thin layer as an electron extraction layer and an approximately 30 nm ZnO thin film measured by AFM was obtained after spin-coated on the top of ITO glass using the method described above. For electron transport layer-based device, an approximately 5 nm thick DPP-COOH or N719 layer was cast on top of ZnO and the film was processed with thermal annealing at 120 ºC for 10 min. Then a solution containing a mixture of P3HT:PCBM (1:1) in dichlorobenzene (DCB) solvent with a fixed concentration of P3HT (10 mg/mL) was spin-cast on top of these films with thickness of approximately 120 nm. The films were heated at 150 ºC for 10 min. Or the PTB7:$PC_{71}BM$ active blend layer, with a nominal thickness of 100 nm was prepared by spin-coating a mixed solvent of chlorobenzene/1,8-diiodoctane (97:3% by volume) solution (concentration, 25 mg/mL) at 1000 rpm for 2 min. For hole transport layer-based device, an approximately 5 nm thick DPP-COOH or N719 layer was cast on top

of active layer and the film was processed with thermal annealing at 120 ºC for 10 min. Then different thickness of MoO_3 layer (6.0 nm) was deposited onto the film surface. Finally, 90 nm Ag were deposited by thermal evaporation through a shadow mask to form an active area of ~4 mm^2.

Characterizations

The nuclear magnetic resonance (NMR) spectra were collected on a Bruker ARX 600 NMR spectrometer with deuterated chloroform as the solvent and with tetramethylsilane (δ=0) as the internal standard. The ultraviolet-visible (UV-Vis) spectra of the samples were recorded on a Perkin Elmer Lambda 750s spectrophotometer. Fluorescence measurement for photoluminescence (PL) of all simples was carried out on a Shimadzu RF-5301 PC spectrofluorophotometer with a xenon lamp as the light source. Time-resolved photoluminescence spectra of the samples were recorded on an Edinburgh FLS920 fluorescence lifetime and standby state spectrometer. Texture observations by polarizing optical microscopy (POM) were made with a Nikon E600POL polarizing optical microscope equipped with an Instec HS 400 heating and cooling stage. Atomic force microscopic (AFM) images were measured by a Agilent 5500 (Digital Instrument) scanning probe microscope using the tapping mode. Transmission electron microscopy (TEM) was employed on JEOL, JEM-2100F (field emission transmission electron microscope). The light source was calibrated by using silicon reference cells with an AM 1.5 Global solar simulator with an intensity of 100 mW/cm^2. The current-voltage (*J-V*) characteristics were recorded using Keithley 2400 Source Meter (Abet Solar Simulator Sun2000). All the measurements were performed under ambient atmosphere at room temperature. The EQE was measured under monochromatic illumination (Oriel Cornerstone 260 1/4 m monochromator equipped with Oriel 70613NS QTH lamp), and the calibration of the incident light was performed with a monocrystalline silicon diode. The light was set using a Newport calibrated filtered Si reference cell.

Ultraviolet photoelectron spectroscopy (UPS)

ZnO thin film was prepared by the method described above. MoO_3, DPP-COOH/MoO_3 and N719/MoO_3 were prepared by deposition of 6 nm MoO_3 thick on the top of hole transport layer. ZnO, ZnO/DPP-COOH and ZnO/N719 thin films were also processed. The UPS measurements were carried out in a Thermo Fisher Scientific Ultra Spectrometer using a He I (21.22 eV) discharge lamp. A bias of -5.0 V was applied to the samples for separation of the sample and the secondary edge for the analyzer. The work function (Φ) was determined by $E_{HOMO} = h\nu - (E_{onset}^{HOMO} - E_{cutoff})$, Where $h\nu$ is the incident photon energy, $h\nu$ =21.22 eV; E_{cutoff} is defined as the lowest kinetic energy of the measured electrons which can be obtained from the UPS measurement; E_{onset}^{HOMO} was the HOMO energy onset, generally referred to as the high kinetic energy onset.

Space-charge-limited-current (SCLC) mobility measurement

To further investigate the effect of the blend film structure on the photovoltaic properties, the hole and electron mobility were detected via the space-charge-limited current (SCLC) method. The electron-only devices used a diode configuration of ITO/Al/P3HT:PCBM/LiF/Al and the hole-only devices was built as ITO/PEDOT:PSS/P3HT:PCBM/MoO_3/Au.[3-5] The carrier mobility was measured using the SCLC model at low voltage which is described by Equation:

$J=9\varepsilon_0\varepsilon_r\mu(V_a-V_{bi})^2/8L^3$

Where J is current density, ε_0 is the permittivity of free space, ε_r is relative permittivity of the material (for conjugated polymer, ε_r is 3 in general), μ is the mobility of electron or hole, V_a is the applied voltage, V_{bi} is built-in voltage, and L is the film thickness. The thickness of the BHJ blend for SCLC measurement was about 120 nm. By fitting the results to a space-charge-limited form, $J^{0.5}$-V was plotted and the carrier mobility were summarized in **Table S1**.

The observed low dark current densities implied that CSMEs used as ETLs for inverted BHJ solar cells possessed larger V_{oc} than those without any ILs. Towards the

end, we modeled the *J-V* characteristics of BHJ solar cells with an equivalent circuit, consisting of a sing diode with series resistance (R_S) and shunt resistance (R_{SH}) in **Table 1** and **Table 2**. The addition of a parallel photocurrent source, J_{ph}, leads to the well-known equation:

$$J = J_0[\exp(\frac{q(V - R_S AJ)}{nkT}) - 1] + \frac{V - R_S AJ}{R_{SH} A} - J_{ph}(V)$$

Where q is the electron charge, k is Boltzmann's constant, T is the temperature, and J_{ph} is the voltage-dependent photocurrent produced by the cell. By rearranging this eq. $E_{HOMO} = hv - (E_{onset}^{HOMO} - E_{cutoff})$ under open circuit condition (J=0) and J_{ph}=J_{sc}, V_{oc} can be described as $V_{oc} \approx \frac{nkT}{q} \ln(\frac{J_{sc}}{J_0})$, where J_o is reverse dark current density. The lower the J_o, the higher the V_{oc}. Therefore, inverted BHJ solar cells with ETLs possessed higher V_{oc} than those with HTLs or without IL.

Reference:

1. W. Shin, T. Yasuda, G. Watanabe, Y. S. Yang, C. Adachi, *Chem. Mater.,* 2013, **25,** 2549.

2. Y. Sun, J. H. Seo, C. J. Takacs. J. Seifter, A. J. Heeger, *Adv. Mater.,* 2011, **23,** 1679.

3. T. Yang, M. Wang, C. Duan, X. Hu, L. Huang, J. Peng, F. Huang, X. Gong, *Energy Environ. Sci.,* 2012, **5,** 8208.

4. A. R. B. M. Yusoff, S. J. Lee, H. P. Kim, F. K. Shneider, W. J. D. Silva, J. Jang, *Adv. Funct. Mater.,* 2013, **24,** 2240.

5. C.-Y. Mei, L. Liang, F.-G. Zhao, J.-T. Wang, L.-F. Yu, Y.-X. Li, W.-S. Li, *Macromolecules,* 2013, **46,** 7920.

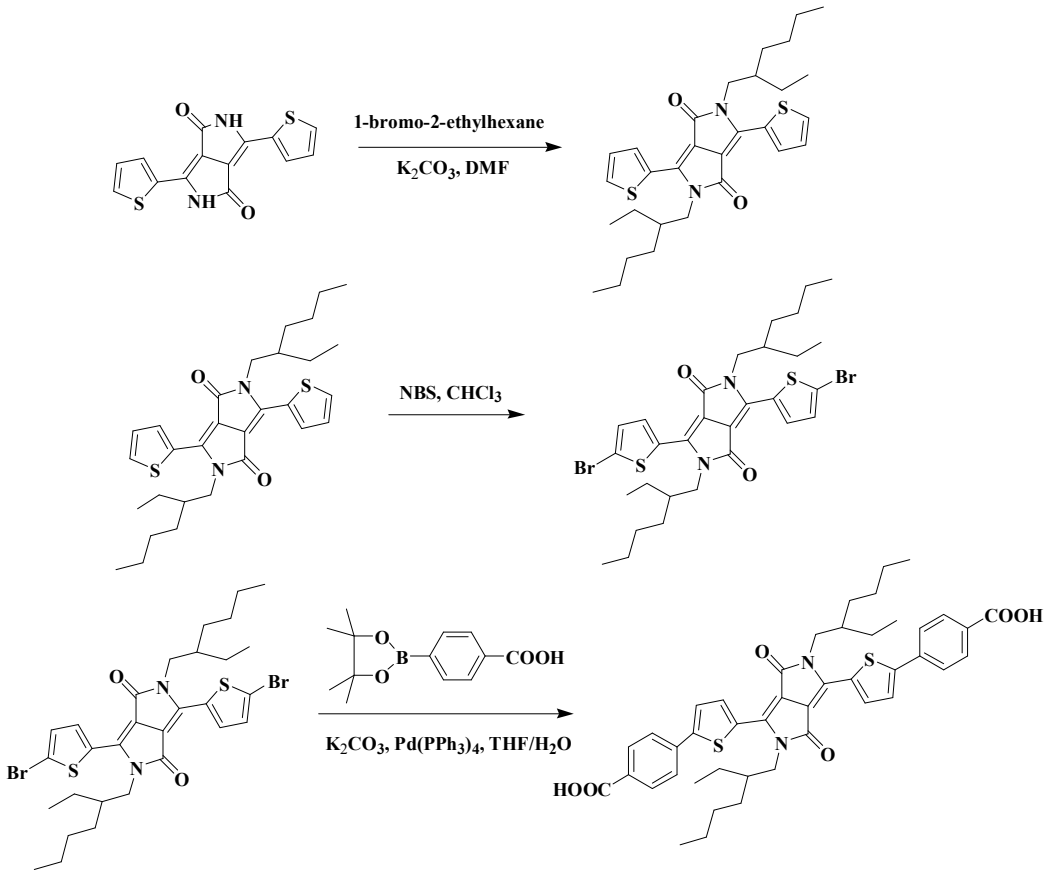

N719:Di-tetrabutylammonium cis-bis(isothiocyanato)bis(2,2′-bipyridyl-4,4′-dicarboxylato)ruthenium (Ⅱ)

DPP-COOH: 3,6-Bis-(5- benzoic acid-thiophen-2-yl)-2,5-bis-(2-ethylhexyl)- 2,5-dihydro-pyrrolo[3,4-*c*]pyrrole-1,4-dione

DPP-COOH: 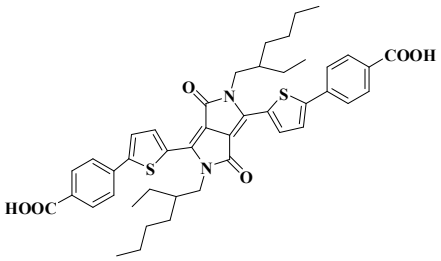

N719: 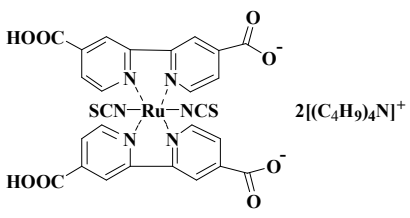

Scheme S1. Synthesis of DPP-COOH molecule as the interfacial layers, the chemical names and structures of DPP-COOH and N719 and the DPP-COOH solution in CH_3OH.

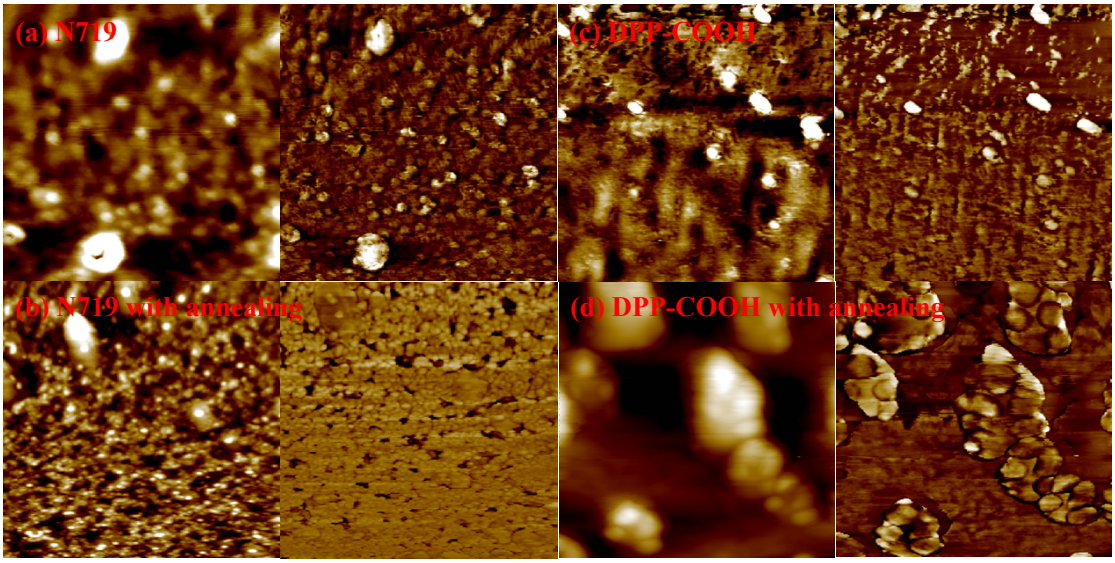

Fig. S1. Tapping-mode atomic force microscopy (AFM) high (left) and phase (right) images: (a), (b) the surface of N719 film without and with thermal annealing at 120 ºC for 10 min, respectively; (c), (d) the surface of DPP-COOH film without and with thermal annealing at 120 ºC for 10 min, respectively. The image sizes were all 5 μm × 5 μm.

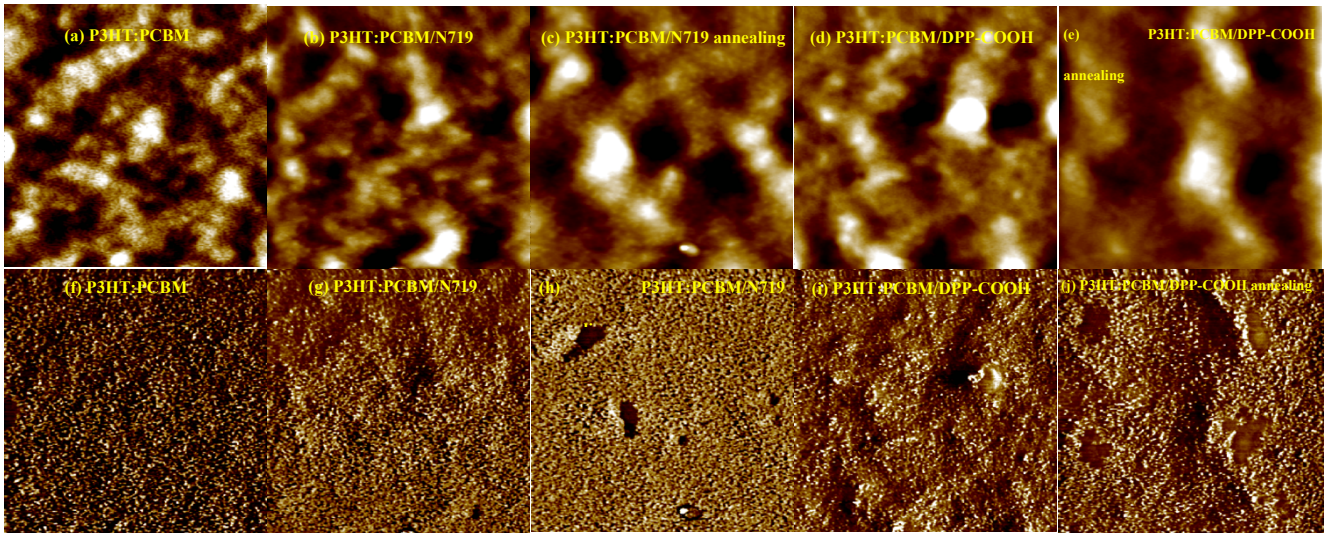

Fig. S2. Tapping-mode atomic force microscopy (AFM) high and phase images: (a), (f) the surface of pristine P3HT:PCBM film; (b), (g) the surface of P3HT:PCBM/N719 film; (c), (h) the surface of P3HT:PCBM/N719 film at 120 ºC annealing for 10 min; (d), (i) the surface of P3HT:PCBM/DPP-COOH film and (e), (j) the surface of P3HT:PCBM/DPP-COOH film at 120 ºC annealing for 10 min. The image sizes were all 5 μm × 5 μm.

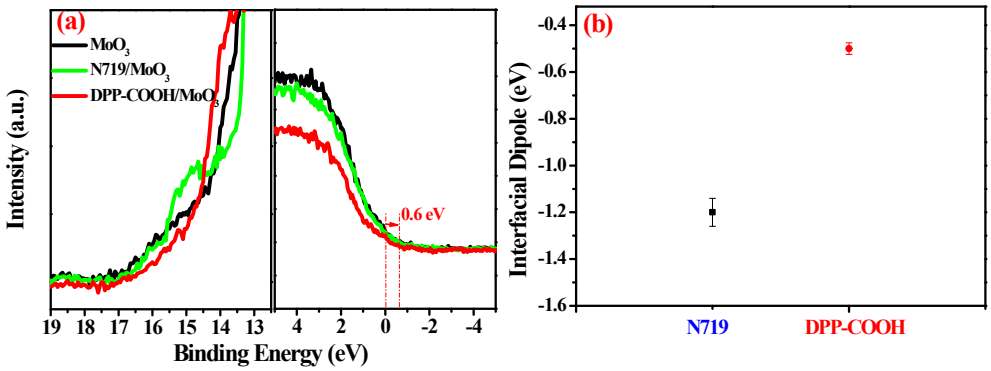

Fig. S3. (a) Ultraviolet photoemission spectra (UPS) of pristine MoO_3, N719/MoO_3 and DPP-COOH/MoO_3; (b) Interfacial dipole energy (Δ) of the two CSMEs on MoO_3.

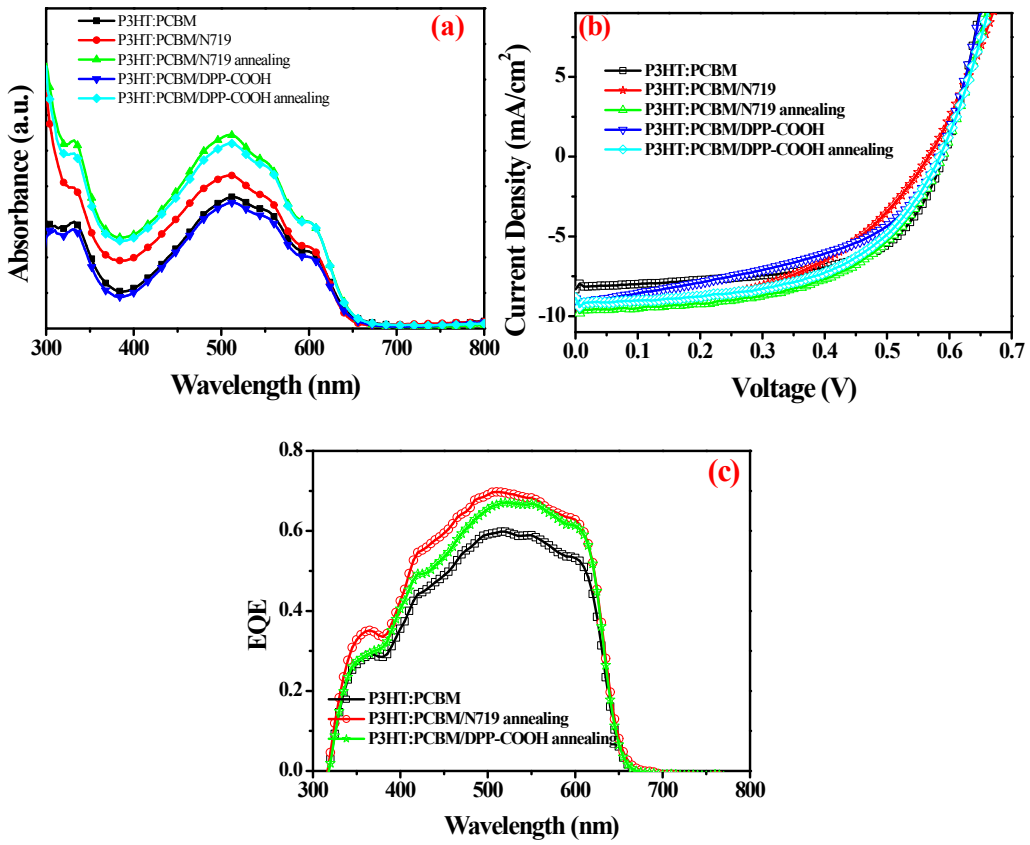

Fig. S4. (a) UV-vis absorption spectra of the similar devices with the different hole transport layer; (b) *J-V* curves of the PSCs based on P3HT:PCBM with N719 and DPP-COOH as anode buffer layer without or with thermal annealing at 120 ºC under illumination of AM 1.5G, 100 mW/cm^2; (c) IPCE versus wavelength for inverted BHJ solar cells with various hole transport layer.

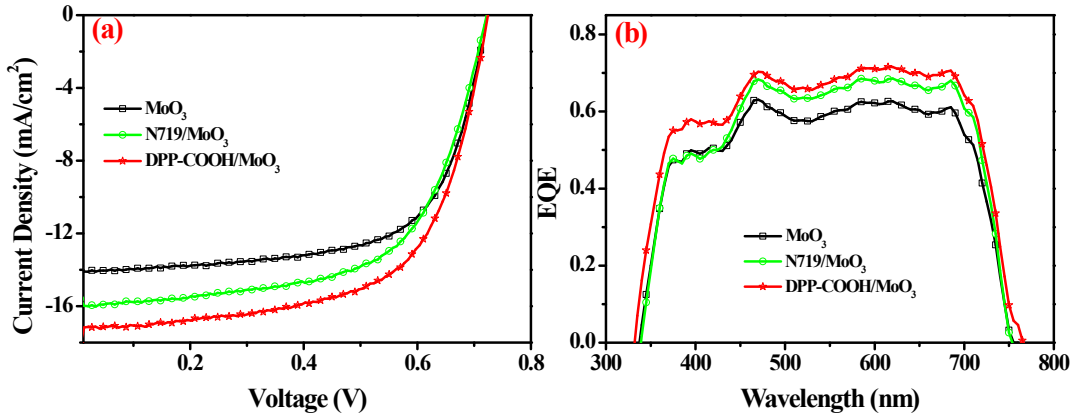

Fig. S5. (a) *J-V* curves of the PSCs based on PTB7:$PC_{71}BM$ with N719 and DPP-COOH as HTLs without thermal annealing under illumination of AM 1.5G, 100 mW/cm^2; (b) External quantum efficiency spectra of PTB7:$PC_{71}BM$ solar cells using DPP-COOH and N719 as HTLs.

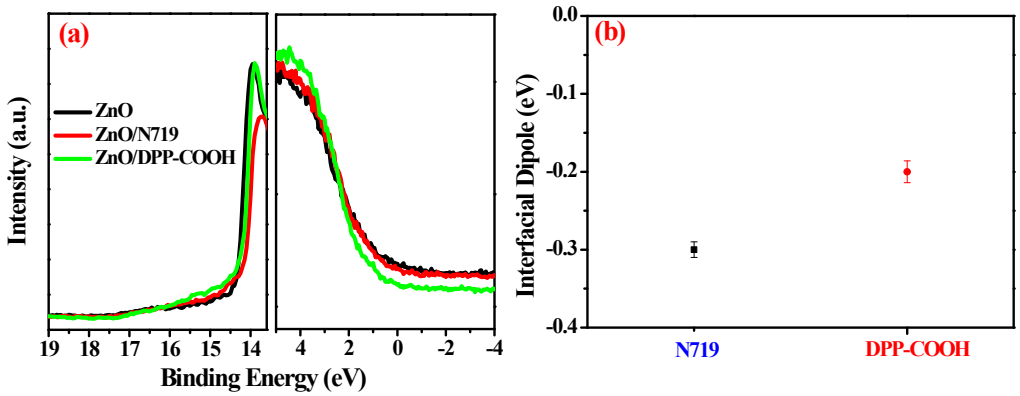

Fig. S6. (a) Ultraviolet photoemission spectra (UPS) of pristine ZnO, ZnO/N719 and ZnO/DPP-COOH; (b) Interfacial dipole energy (Δ) of the two CSMEs on ZnO.

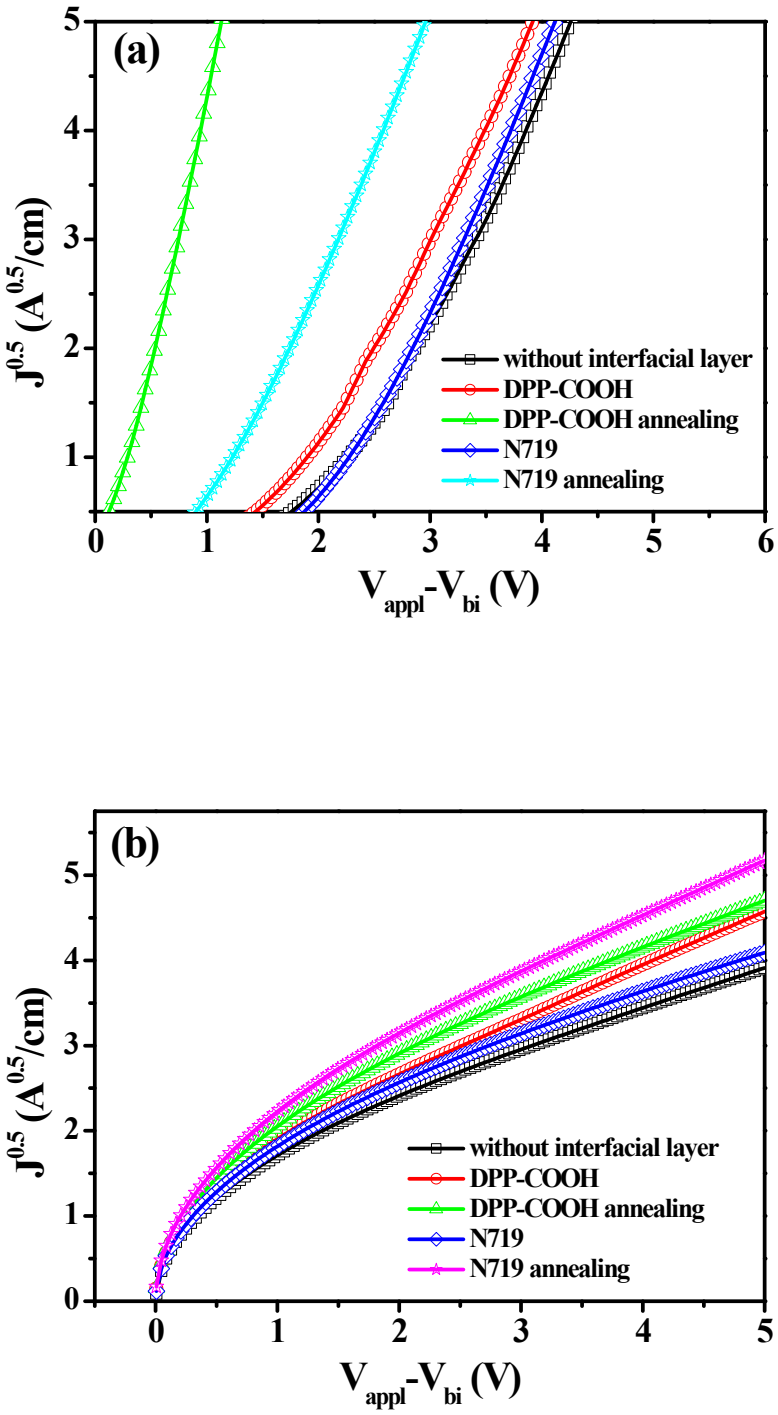

Fig. S7. $J^{0.5}$-V characteristics of (a) electron-only and (b) hole-only devices based on P3HT:PCBM active layer with various interfacial layers with or without thermal annealing.

Table S1. Summary of the carrier mobility of the P3HT:PCBM device with various ETLs.

Interlayer	Electron mobility ($cm^2/V \cdot s$)[a]	Hole mobility ($cm^2/V \cdot s$)[b]
Without interlayer	2.94×10^{-3}	2.74×10^{-4}
DPP-COOH	4.15×10^{-3}	3.53×10^{-4}
DPP-COOH annealing	5.44×10^{-3}	4.01×10^{-4}
N719	3.55×10^{-3}	2.95×10^{-4}
N719 annealing	4.16×10^{-3}	4.92×10^{-4}

[a] Electron-only device configuration: ITO/Al/P3HT:PCBM/LiF/Al. [b] Hole-only device configuration: ITO/PEDOT:PSS/P3HT:PCBM/MoO_3/Au.

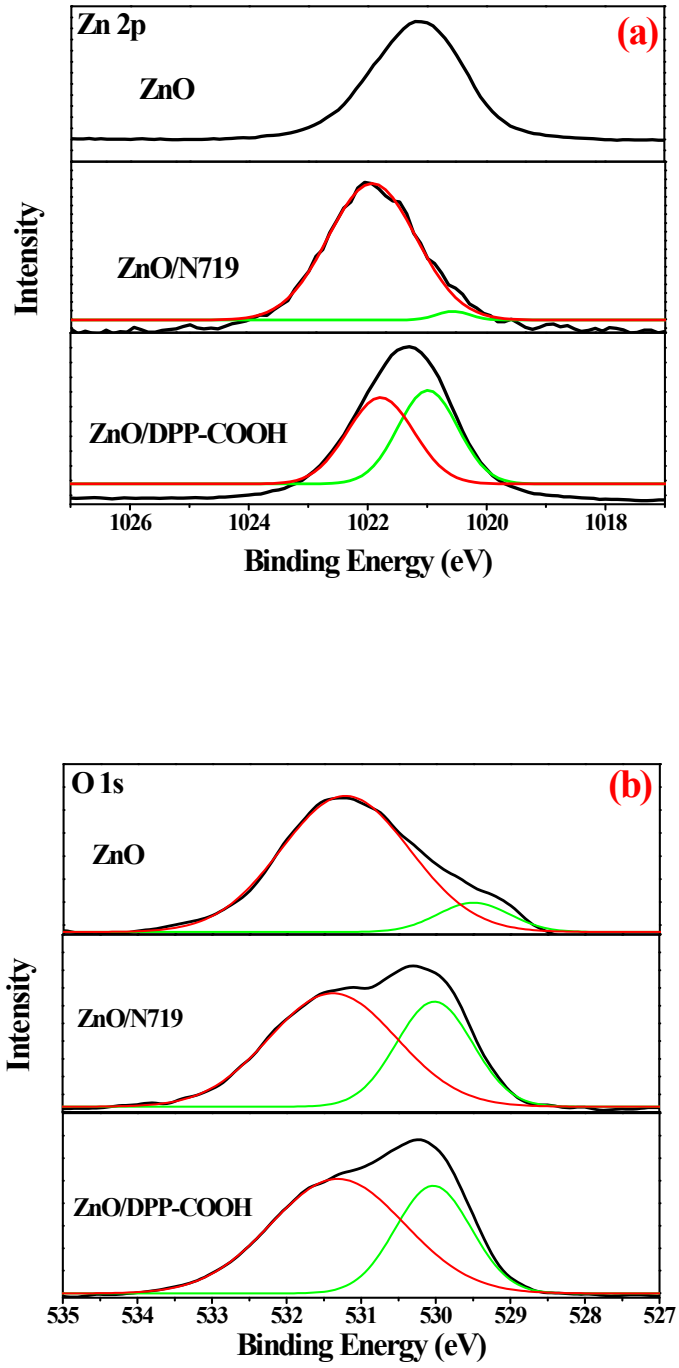

Fig. S8. X-ray photoelectron spectroscopy (XPS) peaks for ZnO, ZnO/N719 and ZnO/DPP-COOH films, (a) Zn 2p and (b) O 1s spectra.

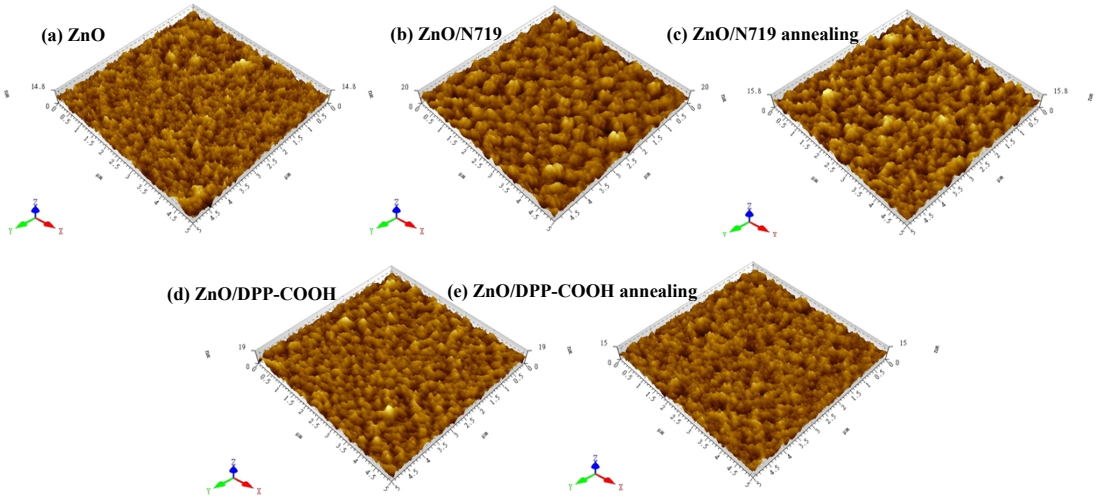

Fig. S9. Three-dimensional atomic force microscopy (AFM) images: (a) pristine ZnO film; (b) ZnO/N719 film; (c) ZnO/N719 film at 120 °C annealing for 10 min; (d) ZnO/DPP-COOH film and (e) ZnO/DPP-COOH film at 120 °C annealing for 10 min. The image sizes were all 5 μm × 5 μm.

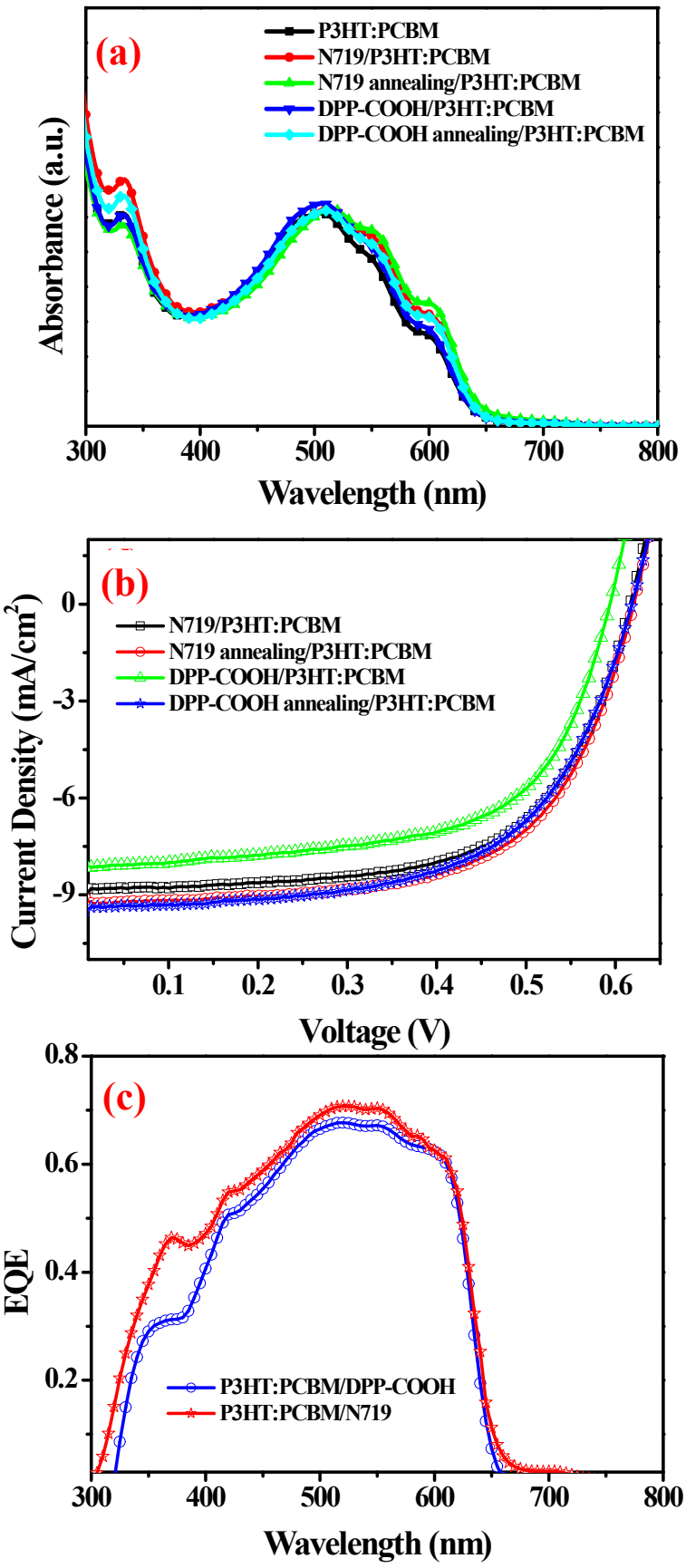
(a)
P3HT:PCBM
N719/P3HT:PCBM
N719 annealing/P3HT:PCBM
DPP-COOH/P3HT:PCBM
DPP-COOH annealing/P3HT:PCBM
Absorbance (a.u.)
300
400
500
600
700
800
Wavelength (nm)
(b)
N719/P3HT:PCBM
N719 annealing/P3HT:PCBM
DPP-COOH/P3HT:PCBM
DPP-COOH annealing/P3HT:PCBM
Current Density (mA/cm2)
0
-3
-6
-9
0.1
0.2
0.3
0.4
0.5
0.6
Voltage (V)
(c)
EQE
0.8
0.6
0.4
0.2
P3HT:PCBM/DPP-COOH
P3HT:PCBM/N719
300
400
500
600
700
800
Wavelength (nm)

Fig. S10. (a) UV-vis absorption spectra of the similar devices with the different electron transport layer; (b) *J-V* curves of the PSCs based on P3HT:PCBM with N719 and DPP-COOH as cathode buffer layer without or with thermal annealing at 120 ºC under illumination of AM 1.5G, 100 mW/cm^2; (c) External quantum efficiency spectra of P3HT:PCBM solar cells using DPP-COOH and N719 as ETL.

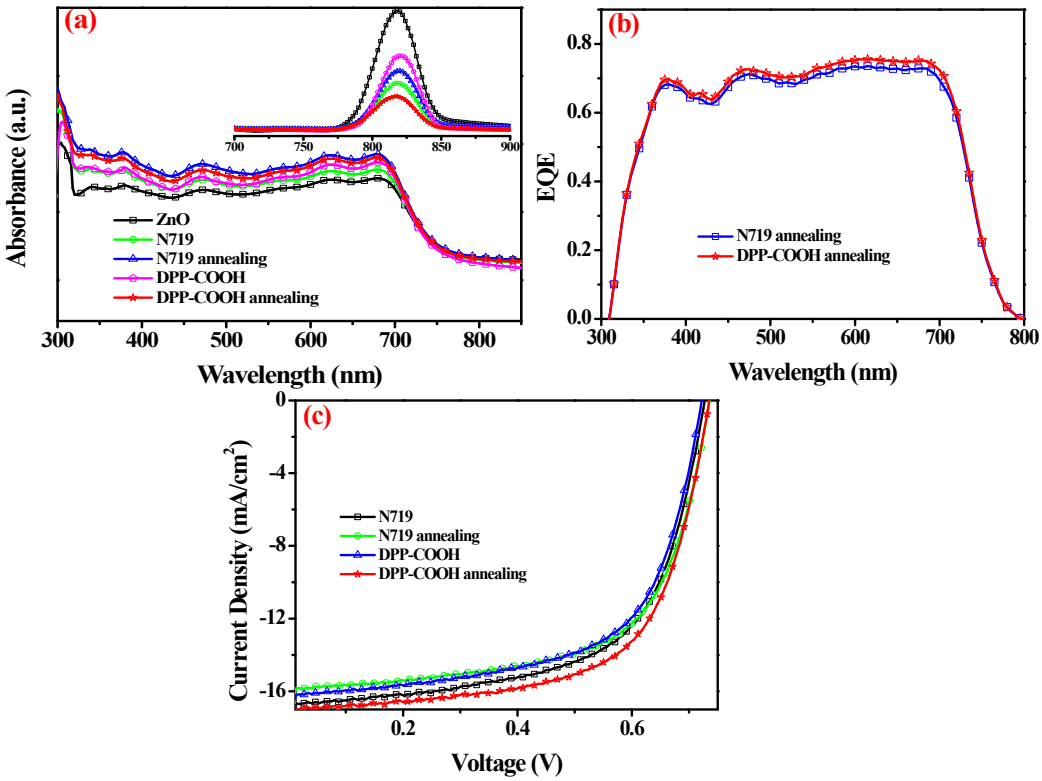

Fig. S11. (a) UV-vis absorption spectra of the similar devices based on PTB7:$PC_{71}BM$ active layer with different ETLs (The inset is the corresponding PL spectra.); (b) External quantum efficiency spectra of PTB7:$PC_{71}BM$ solar cells using DPP-COOH and N719 with thermal annealing at 120 ^{o}C as ETLs; (c) *J-V* curves of the PSCs based on PTB7:$PC_{71}BM$ with N719 and DPP-COOH as ETL with or without thermal annealing at 120 ^{o}C under illumination of AM 1.5G, 100 mW/cm^2.

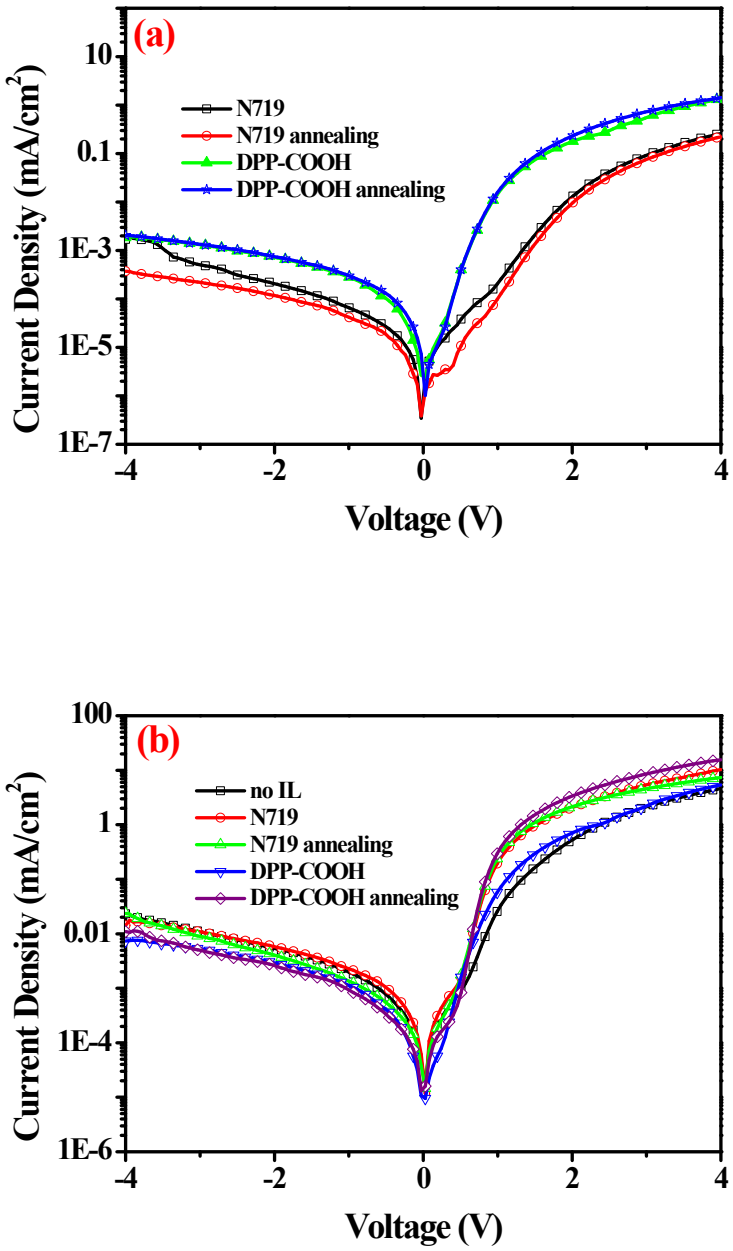

Fig. S12. *J-V* characteristics of inverted BHJ solar cells with device architectures of (a) ITO/ZnO/interfacial layer/PTB7:$PC_{71}BM$/MoO_3/Ag and (b) ITO/ZnO/interfacial layer/PTB7:$PC_{71}BM$/MoO_3/Ag in the dark.

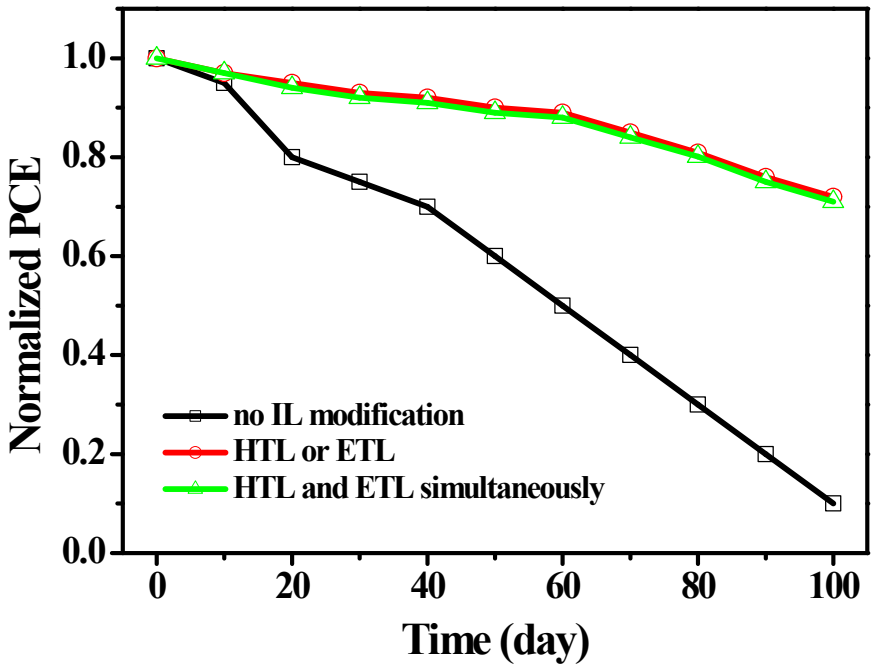

Fig. S13. Normalized PCEs for inverted polymer solar cells with different ILs modifications as a function of storage time in air under ambient conditions.